https://doi.org/10.1007/s11467-023-1292-4

Strongly nonlinear topological phases of cascaded topoelectrical circuits

Jijie Tang[1,*], Fangyuan Ma[2,*], Feng Li[2,†], Honglian Guo[1,‡], Di Zhou[2,#]

[1]College of Science, Minzu University of China, Beijing 100081, China
[2]Centre for Quantum Physics, Key Laboratory of Advanced Optoelectronic Quantum Architecture and Measurement (MOE), School of Physics, Beijing Institute of Technology, Beijing 100081, China
*These authors contributed equally to this work.
Corresponding authors. E-mail: †phlifeng@bit.edu.cn, ‡hlguo@muc.edu.cn, #dizhou@bit.edu.cn
Received January 18, 2023; accepted April 2, 2023

I. METHOD

A. Circuit design

Electrical circuits are built on the printed circuit board (PCB) (thickness, 1.6 mm), with each nonlinear capacitor consisting of a pair of back-to-back varactors (Skyworks Solutions, SMV1255 -011LF). The capacitance ranges from 37.7 pF to 5 pF as the DC voltage changes in the range between 0 to 7V. We use network analyzer and LC series circuit to measure the capacitance curve of the nonlinear capacitor, with the fixed chip capacitors (tolerance, ±5%), the fixed chip inductors (tolerance, ±10%), and the direct insertion resistors (tolerance,±1%).

B. Measurement set-up

The experimental observation of the topological interface mode is performed by measuring the impedance of each point marked as V_n in the circuit system. The method of measuring the impedance is the resistance voltage divider circuit method, as shown in Fig.S1 below. The function signal generator produces the chirp signal and adjusts the amplitude. The frequency of the chirp signal ranges from 0Hz to 33.3MHz.

The amplifier (Minicircuit ZHL-6A-S+) amplifies the chirp signal by the factor of 24.2 dB. We use the oscilloscope (KEYSIGHT DSOX4054A) to collect the data of V_0 and V_n, as shown by the nodes on the two sides of R_0 in Fig. S1. Fourier transformation is performed to obtain the frequency spectrum of the response. The impedance Z_n of each node in the circuit is computed via $Z_n = R_0 \cdot V_n/(V_0 - V_n)$.

II. EQUATIONS OF MOTION OF THE NONLINEAR TOPOELECTRICAL CIRCUIT

In this section, we establish the equations of motion of the cascaded circuit, which is subjected to periodic boundary condition (PBC), and the unit cell is depicted by Fig. S2.

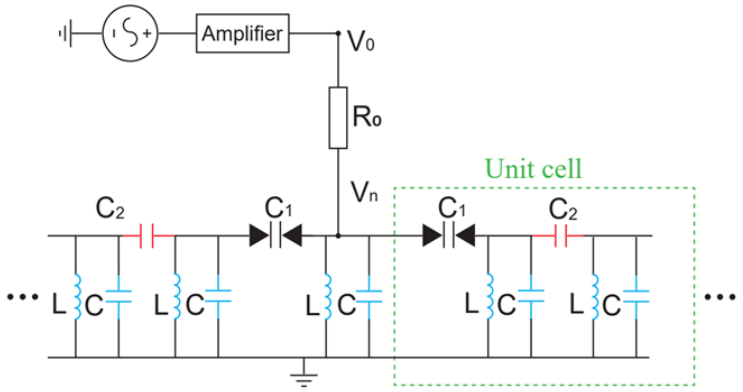

FIG. S1. The method of impedance measurement.

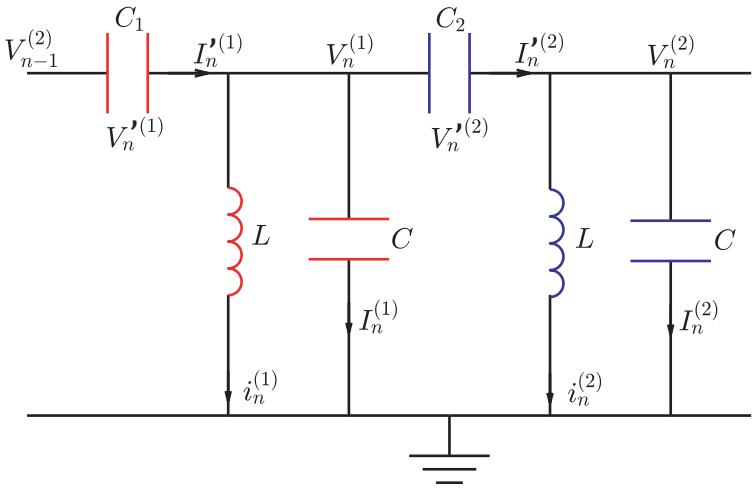

FIG. S2. The unit cell of the nonlinear topoelectrical circuit, where L, C are purely linear inductor and capacitor, respectively, and $C1(V)$, $C2(V)$ are nonlinear capacitors that vary upon the change of the biased voltages.

We conduct the system Lagrangian, from which the nonlinear motion equations are de-rived. The circuit Lagrangian reads

$$\mathrm{L}(\{V_n^{(1)}, V_n^{(2)}\}) = \sum_n \left[\mathrm{L}_n - U_1(V_{n-1}^{(2)} - V_n^{(1)}) - U_2(V_n^{(1)} - V_n^{(2)})\right], \tag{S1}$$

where $V_n^{(1)}$ and $V_n^{(2)}$ denote the voltage fields in the unit cell, $i_n^{(1)}$ and $i_n^{(2)}$ are the currents that flow in the inductances, $\mathrm{L}_n = \frac{1}{2}L(i_n^{(1)2} + i_n^{(2)2}) - \frac{1}{2}C(V_n^{(1)2} + V_n^{(2)2})$ is the Lagrangian of the two LC resonators in the unit cell, and

$$U_{j=1,2}(V) = \int_0^V (V - x)C_{j=1,2}(x) \tag{S2}$$

are the strongly an-harmonic potential energy of the nonlinear capacitors $C_{j=1,2}(V)$.

It is worth emphasizing that the nonlinear capacitors yield even function $C_{j=1,2}(V) = C_{j=1,2}(-V)$ of the biased voltage, because the nonlinear capacitor is composed of back-to-back varactor diodes that intrinsically yields the structural reflection symmetry [1]. Thus, it is straightforward to arrive at the result that the nonlinear potential energy of the capacitor $C_{j=1,2}$ is an even function of the biased voltage, $U_{j=1,2}(V) = U_{j=1,2}(-V)$. In the next section, we will show that together with the diatomic structure of the unit cells, the nonlinear dynamics of the circuit system yields reflection symmetry, which subsequently quantizes the nonlinear Berry phase.

According to Kirchhoff law, we write the currents of the inductances in terms of the currents that flow in the capacitors. Due to the conservation law of the current at every node, we have the relationships

$$\begin{aligned} i_n^{(1)} &= I_n^{\prime(1)} - I_n^{(1)} - I_n^{\prime(2)}, \\ i_n^{(2)} &= I_n^{\prime(2)} - I_n^{(2)} - I_{n+1}^{\prime(1)}. \end{aligned} \tag{S3}$$

Then, the currents in the linear capacitors of the LC resonators are given by

$$I_n^{(j=1,2)} = C\frac{dV_n^{(j=1,2)}}{dt}, \tag{S4}$$

whereas the currents that flow in the nonlinear capacitors read

$$\begin{aligned} I_n^{\prime(1)} &= C_1(V_{n-1}^{(2)} - V_n^{(1)})\left(\frac{dV_{n-1}^{(2)}}{dt} - \frac{dV_n^{(1)}}{dt}\right), \\ I_n^{\prime(2)} &= C_2(V_n^{(1)} - V_n^{(2)})\left(\frac{dV_n^{(1)}}{dt} - \frac{dV_n^{(2)}}{dt}\right). \end{aligned} \tag{S5}$$

Summarizing all these Eqs.(S3, S4, S5), now the system Lagrangian can be expressed only in terms of the voltage fields $V_n^{(j=1,2)}$ and their time-derivatives $\dot{V}_n^{(j=1,2)}$.

Having established the system Lagrangian in terms of the voltage fields, we can now express the nonlinear dynamics of the circuit system using Lagrangian equations motion

$$\frac{d}{dt}\frac{\partial \mathrm{L}}{\partial \dot{V}_n^{(j)}} - \frac{\partial \mathrm{L}}{\partial V_n^{(j)}} = 0 \qquad \text{for} \qquad j = 1, 2. \tag{S6}$$

Despite that the nonlinear dynamics of the voltage fields $V_n^{(j=1,2)}$ appear second-order derivative in time, one can convert them as the first-order time derivatives by defining

$$\Psi_n = (\Psi_n^{(1)}, \Psi_n^{(2)}, \Psi_n^{(3)}, \Psi_n^{(4)}) = (V_n^{(1)}, -\mathrm{i}\dot{V}_n^{(1)}, V_n^{(2)}, -\mathrm{i}\dot{V}_n^{(2)}) \tag{S7}$$

as the classical field variable of the nth unit cell. By doing so, one converts the circuit dynamics as the four-field generalized nonlinear Schrödinger equations.

III. NONLINEAR EXTENSION OF BLOCH THEOREM

Spatially repetitive structures enjoy the nice property of discrete translational symmetry, meaning that the system Lagrangian as well as the nonlinear equations of motion are invariant for translational operations. As a result, spatial-temporal periodic modes in the system take the format of plane-wave nonlinear normal modes [2–4]. For example, plane-wave voltage fields of the circuit system yields the format of $V_k(t) = (V_k^{(1)}(\omega t - kn), V_k^{(2)}(\omega t - kn + \phi_k))$, where k and ω are the wavenumber and frequency, respectively, and ϕ_k characterizes the phase difference between these two wave components. Likewise, the plane-wave format of the four-component classical field reads

$$\Psi_k(t) = (\Psi_k^{(1)}(\omega t - kn + \phi_k^{(1)}), \Psi_k^{(2)}(\omega t - kn + \phi_k^{(2)}), \Psi_k^{(3)}(\omega t - kn + \phi_k^{(3)}), \Psi_k^{(4)}(\omega t - kn + \phi_k^{(4)})), \quad \text{(S8)}$$

where $\Psi_k^{j=1,2,3,4}$ are 2π-periodic wave components, and the phase conditions are chosen by asking that $\mathrm{Re}\,\Psi_k^{(j)}(\theta = 0) = \max(\mathrm{Re}\,\Psi_k^{(j)})$ reaches the maximum of the wave component at $\theta = 0$. Thus, $\phi_k^{(j=1,2,3,4)}$ characterize the relative phase of each wave component.

To prove the nonlinear extension of Bloch theorem, we consider a temporal-periodic solution of the nonlinear circuit, denoted as $\Psi_n(\omega t)$, where ω is the mode frequency. The mode follows the equations of motion in Eq.(S6), and the corresponding system Lagrangian is $\mathrm{L}(\Psi_n(\omega t))$. Due to the discrete translational symmetry of the underlying circuit lattice, it is natural to find a partner nonlinear solution $\tilde{\Psi}_n(\omega t)$, which yields $\tilde{\Psi}_{n+1}(\omega t) = \Psi_n(\omega t)$. $\tilde{\Psi}_n(\omega t)$ also satisfies the nonlinear equations of motion as the system Lagrangian stays invariant via $\mathrm{L}(\tilde{\Psi}_n(\omega t)) = \mathrm{L}(\Psi_n(\omega t))$. As there is no degeneracy of nonlinear normal modes, the nonlinear solutions $\tilde{\Psi}_n(\omega t)$ and $\Psi_n(\omega t)$ have to be the same solution. Therefore, they can only differ by a phase factor $\Delta\theta$, with $\tilde{\Psi}_n(\omega t + \Delta\theta) = \Psi_n(\omega t)$, which further leads to $\tilde{\Psi}_n(\omega t + \Delta\theta) = \tilde{\Psi}_{n+1}(\omega t)$. We translate the lattice position of the nonlinear wave function $\tilde{\Psi}_n(\omega t)$ by N times, to find $\tilde{\Psi}_n(\omega t + N\Delta\theta) = \tilde{\Psi}_{n+N}(\omega t) \overset{\mathrm{PBC}}{=} \tilde{\Psi}_n(\omega t)$. This imposes the constraint $N\Delta\theta = 2m\pi$ with $m = 0, 1, 2, \ldots, N-1$. Finally, we dub $k = \Delta\theta = 2m\pi/N$ the wave number of the plane-wave nonlinear normal mode. It is at this point that we demonstrate the nonliner extension of Bloch theorem.

IV. REFLECTION SYMMETRY AND QUANTIZED BERRY PHASE

This section aims to construct the nonlinear Berry phase of plane-wave nonlinear normal modes, reveal the reflection symmetry of the circuit dynamics, and demonstrate the topological invariance of nonlinear Berry phase.

Beginning from the plane-wave nonlinear normal mode in Eq.(S8), we realize the adiabatic evolution of the wavenumber $k(t')$ by allowing it to traverse through the Brillouin zone, from $k(0) = k$ to $k(t) = k + 2\pi$, while the amplitude A of the nonlinear voltage fields in the circuit remains unchanged during this process. According to the nonlinear extension of the adiabatic theorem [5–8], a system $H(\Psi_k)$ initially in one of the nonlinear modes Ψ_k will stay as an instantaneous nonlinear mode of $H(\Psi_{k(t)})$ throughout this procedure. Therefore, the only degree of freedom is the phase of mode. At time t, the mode is $\Psi_{k(t)}(\int_0^t \omega(t', q(t'))dt' - \gamma(t))$, where $\gamma(t)$ defines the phase shift of the plane-wave nonlinear normal mode in the adiabatic evolution. The dynamics of γ follows from

$$\frac{d\gamma}{dt}\frac{\partial \Psi_k}{\partial \theta} = \frac{dk}{dt}\frac{\partial \Psi_k}{\partial k}. \tag{S9}$$

After k traverses the Brillouin zone, the wave function acquires an extra phase γ, which we call Berry phase of nonlinear normal modes,

$$\gamma = \oint_{\mathrm{BZ}} dk \frac{\sum\limits_{l,j=1,2,3,4} \left(l \left| \psi_{l,k}^{(j)} \right|^2 \partial_k \phi_k^{(j)} + i \psi_{l,k}^{(j)*} \partial_k \psi_{l,k}^{(j)} \right)}{\sum\limits_{l',j'=1,2,3,4} l' \left| \psi_{l',k}^{(j')} \right|^2}. \tag{S10}$$

where $j, j' = 1, 2, 3, 4$ denote the four wave components of the classical field Ψ_k, and $\psi_{l,k}^{(j)} = (2\pi)^{-1} \int_0^{2\pi} e^{\mathrm{i}l\theta} \Psi_k^{(j)}$ is the lth Fourier component of $\Psi_k^{(j)}$. We note that in the linear limit, nonlinear Berry phase naturally reduces to the traditional format of linear Berry phase, $\gamma = \oint_{\mathrm{BZ}} dk\, \mathrm{i} \langle \Psi_k | \partial_k | \Psi_k \rangle$.

In a general nonlinear dynamics without any symmetry constraints, γ is not quantized and can take any values between 0 and π. However, the underlying nonlinear circuit structure yields reflection symmetry, which subsequently quantizes the Berry phase of nonlinear normal modes. Below we first show that the system Lagrangian is invariant under reflection transformation, and then demonstrate the quantization of the nonlinear Berry phase.

The second-order time derivative of the voltage dynamics, or equivalently the four-field generalized nonlinear Schrödinger equations, are subjected to reflection symmetry. Under

reflection transformation

$$\mathcal{M}(V_n^{(1)}, V_n^{(2)}) = (V_{-n}^{(2)}, V_{-n}^{(1)}), \tag{S11}$$

the system Lagrangian stays invariant via

$$\mathrm{L}(\{V_n^{(1)}, V_n^{(2)}\}) = \mathrm{L}(\{V_{-n}^{(2)}, V_{-n}^{(1)}\}). \tag{S12}$$

Thus, the Lagrangian equations of motion are also invariant under the reflection transformation. Similarly, the four-field generalized nonlinear Schrödinger equations also stay invariant under the reflection transformation of the classical field variable,

$$\mathcal{M}(\Psi_n^{(1)}, \Psi_n^{(2)}, \Psi_n^{(3)}, \Psi_n^{(4)}) = (\Psi_{-n}^{(3)}, \Psi_{-n}^{(4)}, \Psi_{-n}^{(1)}, \Psi_{-n}^{(2)}). \tag{S13}$$

Thus, given a plane-wave nonlinear normal mode Ψ_k, reflection symmetry guarantees a partner solution

$$\mathcal{M}\Psi_k = (\Psi_k^{(3)}(\omega t + kn + \phi_k^{(3)}), \Psi_k^{(4)}(\omega t + kn + \phi_k^{(4)}), \Psi_k^{(1)}(\omega t + kn + \phi_k^{(1)}), \Psi_k^{(2)}(\omega t + kn + \phi_k^{(2)})) \tag{S14}$$

with the frequency ω and wave number $-k$. On the other hand, a plane-wave nonlinear normal mode of the wavenumber $-k$ and frequency ω is by definition denoted as

$$\Psi_{-k} = (\Psi_{-k}^{(1)}(\omega t + kn + \phi_{-k}^{(1)}), \Psi_{-k}^{(2)}(\omega t + kn + \phi_{-k}^{(2)}), \Psi_{-k}^{(3)}(\omega t + kn + \phi_{-k}^{(3)}), \Psi_{-k}^{(4)}(\omega t + kn + \phi_{-k}^{(4)})) \tag{S15}$$

As there is no degeneracy of the nonlinear normal modes, Ψ_{-k} and $\mathcal{M}\Psi_k$ have to be the same nonlinear mode, which in turn imposes the constraints

$$\phi_k^{(4)} - \phi_k^{(3)} = \phi_{-k}^{(2)} - \phi_{-k}^{(1)}, \qquad \phi_k^{(1)} - \phi_k^{(3)} = \phi_{-k}^{(3)} - \phi_{-k}^{(1)}, \tag{S16}$$

and

$$\Psi_k^{(1)} = \Psi_{-k}^{(3)}, \qquad \Psi_k^{(2)} = \Psi_{-k}^{(4)}. \tag{S17}$$

Eqs.(S16) and (S17) are the mathematical formulation of reflection symmetry in the nonlinear circuit dynamics.

Employing Eqs.(S16) and (S17) gives us the quantization of nonlinear Berry phase in Eq.(S10),

$$\gamma = \frac{1}{2}\oint_{\mathrm{BZ}} dk \frac{\partial}{\partial k}(\phi_k^{(3)} - \phi_k^{(1)}) = 0 \text{ or } \pi \mod 2\pi. \tag{S18}$$

In the last step of Eq.(S18), we employ the constraint from Eq.(S16): at time-reversal-invariant-momenta $k = 0, \pi$, both $\phi_\pi^{(3)} - \phi_\pi^{(1)}$ and $\phi_0^{(3)} - \phi_0^{(1)} = 0$ or π. It is at this point that we demonstrate the topological nature of the nonlinear Berry phase when reflection symmetry is considered. Furthermore, we note that the first and third components of Ψ_n are the voltage fields, i.e., $\Psi_n^{(1)} = V_n^{(1)}$ and $\Psi_n^{(3)} = V_n^{(2)}$, and the second and fourth components of Ψ_n are simply defined from the voltage fields via $\Psi_n^{(2)} = -\mathrm{i}\dot{V}_n^{(1)}$ and $\Psi_n^{(4)} = -\mathrm{i}\dot{V}_n^{(2)}$. Thus, the topological index can be equivalently expressed as the following form,

$$\gamma = \oint_{\mathrm{BZ}} dk \frac{\sum\limits_{l} \left(l \left| v_{l,k}^{(j)} \right|^2 \partial_k \phi_k + \sum\limits_{j=1,2} \mathrm{i} v_{l,k}^{(j)*} \partial_k v_{l,k}^{(j)} \right)}{\sum\limits_{l',j'=1,2} l' \left| v_{l',k}^{(j')} \right|^2} = \phi_\pi - \phi_0 = n\pi, \tag{S19}$$

which is the topological number presented in the main text. Here, ϕ_k denotes the relative phase between the two components of plane-wave nonlinear voltage waves.

As indicated by Eq.(S19), the topological number can experience phase transition as ϕ_π and ϕ_0 jump abruptly between 0 and π for growing amplitudes. These relative phases are determined by comparing the frequencies $\omega(\phi_k = 0)$ and $\omega(\phi_k = \pi)$ for time-reversal-invariant-momenta $k = 0$ and π. $\gamma = \pi$ if $\omega(\phi_0 = 0)$ and $\omega(\phi_\pi = \pi)$ belong to the same nonlinear band, whereas $\gamma = 0$ if $\omega(\phi_0 = 0)$ and $\omega(\phi_\pi = 0)$ are in the same nonlinear band. γ encounters a topological phase transition induced by the critical amplitude $A = A_c$ if the frequencies of upper and lower bands merge at

$$\omega(\phi_\pi = 0, A_c) = \omega(\phi_\pi = \pi, A_c). \tag{S20}$$

We perform the numerical analysis by computing the frequencies of the plane-wave nonlinear normal modes at time-reversal-invariant-momentum $k = \pi$ for a list of increasing amplitudes A. By comparing the frequencies of nonlinear normal modes with odd ($\phi_\pi = \pi$) and even ($\phi_\pi = 0$) parities, we use Eq.(S20) to numerically compute the topological phase transition amplitude A_c.

V. THE NUMERICAL SIMULATION OF PROTOTYPE IN FIG.3 WITH ZERO RESISTANCE

In Fig.S3, the sharp and bright color at 18.86 MHz indicates that the response function on the open boundary is a delta-function, which stems from the standing bulk eigenmode. By

comparing Fig.S3 with Fig.3(f-h), it is evident that the sharp response function is broadened into a Lorentzian form, whose half-width is proportional to the resistance. Consequently, the broadened response function leads to the "leakage" of standing bulk states into the band gap, and the leaked state has a spatial decay rate that is proportional to the resistance. This gives rise to the edge-like behavior that is observed in Fig.3(c-h), experimentally and numerically.

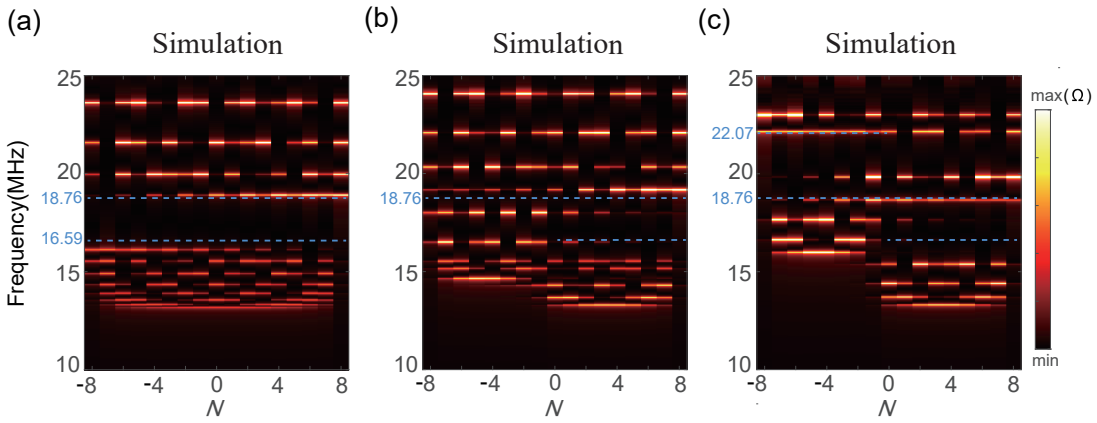

FIG. S3. Numerical simulations of the prototype in Fig.3(a), where the circuit resistance is set to zero. (a-c) Numerical simulations of Fig.3(c-e) respectively.

[1] Y. Wang, L.-J. Lango, C. H. Lee, B. Zhang, and Y.-D. Chong, Topologically enhanced harmonic generation in a nonlinear transmission line metamaterial, Nat. Commun. **10**, 1102 (2019).

[2] D. Zhou, D. Zeb Rocklin, M. Leamy, and Y. Yao, Topological Invariant and Anomalous Edge Modes of Strongly Nonlinear Systems, Nature Communications **13**, 3379 (2022).

[3] M. D. Fronk and M. J. Leamy, Higher-order dispersion, stability, and waveform invariance in nonlinear monoatomic and diatomic systems, Journal of Vibration and Acoustics **139** (2017).

[4] R. K. Narisetti, M. J. Leamy, and M. Ruzzene, A perturbation approach for predicting wave propagation in one-dimensional nonlinear periodic structures, Journal of Vibration and Acous-tics **132** (2010).

[5] D. Xiao, M.-C. Chang, and Q. Niu, Berry phase effects on electronic properties, Rev. Mod. Phys. **82**, 1959 (2010).

[6] J. Liu, B. Wu, and Q. Niu, Nonlinear evolution of quantum states in the adiabatic regime, Phys. Rev. Lett. 90, 170404 (2003).

[7] H. Pu, P. Maenner, W. Zhang, and H. Y. Ling, Adiabatic condition for nonlinear systems, Phys. Rev. Lett. 98, 050406 (2007).

[8] J. Liu and L. B. Fu, Berry phase in nonlinear systems, Phys. Rev. A 81, 052112 (2010).